DRIFT CURRENT UNDER THE ACTION OF WIND AND WAVES

Mohamed Youssef and Malcolm Spaulding
Department of Ocean Engineering
University of Rhode Island
Narragansett, Rhode Island 02882

ABSTRACT

Accurate estimates of sea surface drift currents are critical to forecasting oil spill transport and fate. The majority of existing spill models employ a drift factor and deflection angle, based on local wind speed, to estimate the sea surface drift vector. The effects of wind induced shear and wave induced transport are lumped together in this formulation. In the present approach the conservation of momentum, water mass, and turbulent energy equations are solved using an implicit finite difference method to predict the vertical distribution of current, turbulent energy, and eddy viscosity at one point. The model includes coupling between the wave and shear induced currents. Input energy from the atmosphere to the turbulent energy and current fields are represented through free surface boundary conditions. The numerical model showed excellent agreement in comparison to an analytic solution of the wind forced shear flow problem. The model was applied to predict surface drift currents for varying wind speeds and predicted results in general agreement with field observations and other numerical and theoretical studies. The model predicted drift factor, F, (%) and deflection angle, θ, (degrees) decrease with increasing wind speed, W, (m/s) and can be approximated by the following curve fits:

$F = 3.91 - .0318W$, $\theta = 23.627 - 7.97 \log W$.

The model was applied to three intentional oil spills performed on the Norwegian continental shelf in 1991 and predicted the observed trajectories with reasonable accuracy.

INTRODUCTION

Accurate estimates of the sea surface wind induced drift currents are critical to forecasting oil spill transport and fate. The majority of existing spill models employ an empirically based drift factor and deflection angle, dependent on local wind speed, to estimate the wind and wave induced sea surface drift (Stolzenbach, et al., 1977; Samuels, et al., 1982; Huang and Monastero, 1982; Spaulding, 1988). The drift speed is typically 2.5 to 4% of the wind speed with a mean value of 3.5%. The

where z is the vertical coordinate measured vertically upward from the sea surface, u and v are the x and y Eulerian mean drift velocity components, (subscripts c and w indicate components due to current and wave, respectively), u_s and v_s are the x and y Lagrangian wave drift velocity components, t is time, ρ is density, f is the Coriolis parameter ($2\Omega\sin\phi$), Ω is the angular velocity of the earth's rotation, ϕ is latitude, (positive when north of the equator), and υ is the vertical eddy viscosity coefficient.

In formulating these equations the following were also assumed: The mean total velocity varies slowly relative to the wave period. The wave period is large compared to the characteristic turbulent time scale. The current and wave induced Reynolds stresses can be expressed in terms of the mean Eulerian current and the Lagrangian mean wave drift current, respectively. The molecular viscosity has been neglected compared to its turbulent counterpart.

The conservation of water mass is expressed as

$$\frac{\partial(u_c+u_w)}{\partial x}+\frac{\partial(v_c+v_w)}{\partial y}=0 \qquad (3)$$

The turbulent kinetic energy, $b_c(z,t)$, balance is expressed by the one equation turbulence model

$$\frac{\partial b_c}{\partial t}=\upsilon\left[\left(\frac{\partial u_c}{\partial z}\right)^2+\left(\frac{\partial v_c}{\partial z}\right)^2\right]+\beta\frac{\partial}{\partial z}\left(\upsilon\frac{\partial b_c}{\partial z}\right)-\varepsilon+Q \qquad (4)$$

The first term on the right-hand side of the equation represents turbulence production due to the current shear, the second the vertical diffusion of turbulent energy and the third the dissipative loss, ε. β is a constant (0.73; Davies and Jones,1988) that scales the vertical diffusive transport. A turbulence scaling law, based on Leendertse and Liu (1978) and Davies and Jones (1988), is used to parameterize ε. The last term, Q, represents the turbulent energy production due to wave-current interaction and is expressed as

$$Q=\upsilon\left[\left(\frac{\partial u_s}{\partial z}\right)\left(\frac{\partial u_c}{\partial z}\right)+\left(\frac{\partial v_s}{\partial z}\right)\left(\frac{\partial v_c}{\partial z}\right)\right] \qquad (5)$$

The influence of Coriolis forces was neglected in Equation 4.

To close the system of equations the wave induced currents must be specified. Following Stokes (1847) the Lagrangian mean wave drift is given by

$$u_s = \omega k a^2 e^{2kz} \tag{10}$$

where a is the wave amplitude, k the wave number, ($2\pi/\lambda$, where λ is the wave length) and ω the radian frequency.

The Eulerian mean drift, following Dean and Dalrymple (1984), is given by

$$u_w = \frac{1}{2} \omega k a^2 \tag{11}$$

For a fully-developed sea the wave length can be related to the wind speed (Weber, 1983) by

$$\lambda = (2.803 \times 10^{-3} U_{19.5}^2) \qquad \text{(cm)} \tag{12}$$

where $U_{19.5}$ is the wind speed 19.5 m above sea level in cm/s. This can be related to wind speed at 10 m height, U_{10}, by

$$U_{19.5} = U_{10} \left[1 + \left(c_{10}^{1/2} / \kappa\right) \ln (19.5/10)\right] \tag{13}$$

where c_{10} is the drag coefficient given by Weber (1983)

$$c_{10} = 1.8 \times 10^{-3} \qquad U_{10} < 15 \text{ m/s} \tag{14a}$$

$$c_{10} = 2.7 \times 10^{-3} \qquad U_{10} > 20 \text{ m/s} \tag{14b}$$

The values of c_{10} for U_{10} between 15 and 20 m/s are calculated using linear interpolation. The wind shear stress, τ, is defined as

$$\tau = \rho_a c_{10} U_{10}^2 \tag{15}$$

where ρ_a is the density of air. The radian frequency of the waves, ω, is calculated using the dispersion relation (Dean and Dalrymple, 1984)

$$\omega^2 = kg \tanh kh \tag{16}$$

where g is the gravitational acceleration and h is the mean water column depth. Note that Equation 16 represents the dispersion

m were assumed. The wave drift was specified using Stokes relation. The values of the roughness length, z_0, are based on the experimental results of Wu (1983). At a wind speed of 1 m/s the roughness length is 10^{-2} mm. The roughness length increases rapidly asymptotically approaching a constant value of 5 mm at wind speeds greater than 5 m/s.

A logarithmic transformation of the vertical coordinate was used to obtain finer resolution near the sea surface and increasingly coarser resolution with depth (N=100). The grid spacing increased from 5 mm near the surface to 200 m at the bottom with a resolution of 40 cm at a depth of 10 m. The model time step was 100 seconds. Although the numerical scheme is unconditionally stable the time step was selected to provide accurate predictions for the chosen grid size.

The temporal evolution of the total surface drift current for different wind speeds is shown by the hodographs in Figure 1, where the points on the curve denote hourly values of the nondimensional velocity components. The velocities were nondimensionalized using the surface friction velocity. The results are consistent with Weber's (1983) and Jenkins' (1987) models and show that within the first hour the drift current is predominantly in the direction of the wind. It is evident from the figure that the drift current generates a spiral motion. Initially inertial oscillations are damped very quickly. As time increases the damping decreases significantly and the current asymptotically approaches a steady value. The higher the wind speed the faster the current approaches steady state.

The profiles for the horizontal velocity components near steady state, for wind speeds of 1 and 10 m/s are shown in Figure 2. The vertical coordinate has been nondimensionalized with the water column depth. The figure clearly shows a high velocity shear region near the surface, consistent with field observations (Ambjorn, 1983), which decreases rapidly with ~~increasing~~ depth. The figure also shows that the lower the wind speed the higher the shear. This is due to the combined effect of Stokes drift and low surface eddy viscosity. The change in the velocity profile near the sea surface for 1 m/s wind (Figure 2a) is due to the very high gradient of Stokes drift (Figure 3) and the sudden change in the eddy viscosity profile (Figure 4).

Figure 3 shows the ratio between the Stokes drift velocity at a selected depth and the Stokes drift velocity at the surface versus wind speed. The ratio is representative of the velocity shear. An increase in the ratio implies an increase in the shear. The figure

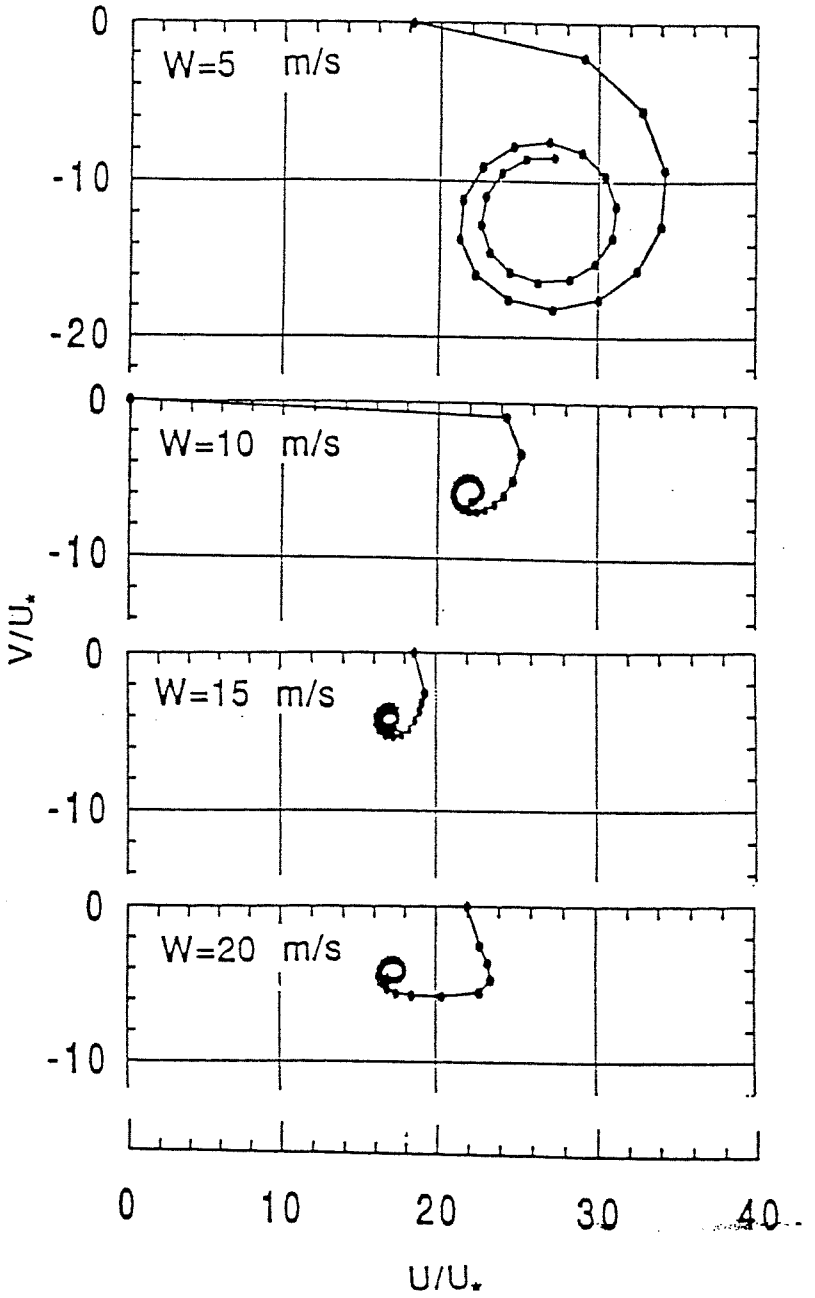

Figure 1 Continued.

which in turn increases the downward momentum diffusion. The wind drift factor therefore decreases and approaches a value of 3% at a wind speed of 30 m/s. Observational data (Samuels, et al., 1982) show a similar trend; the lower the wind speed the higher the wind drift factor. The discontinuous behavior of the drift factor at 15 m/s is caused by the change in the value of the friction factor used in the wind stress formulation (Weber, 1983; Jenkins, 1987) (Equation 14).

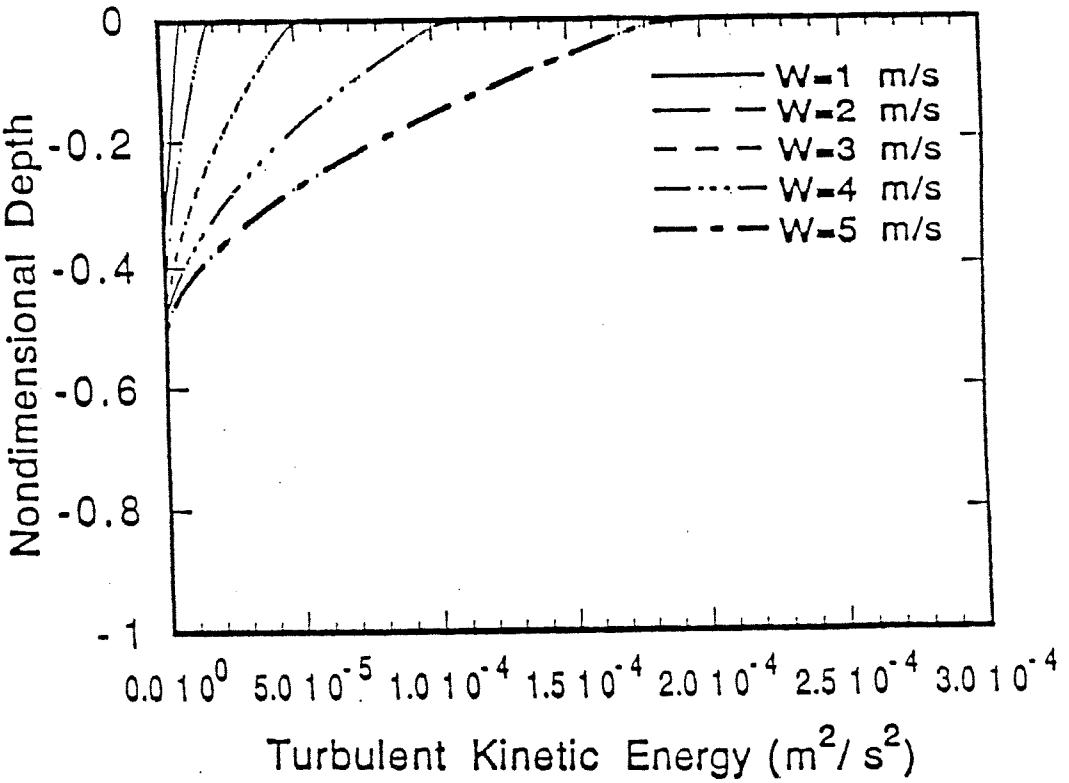

Figure 5 Steady-state turbulent kinetic energy profiles for different wind speeds.

To provide a simple approximation of the dependence of drift factor on wind speed the model predictions (Figure 6) were curve fit and give the following expression

$$F = 3.91 - .0318W \qquad (17)$$

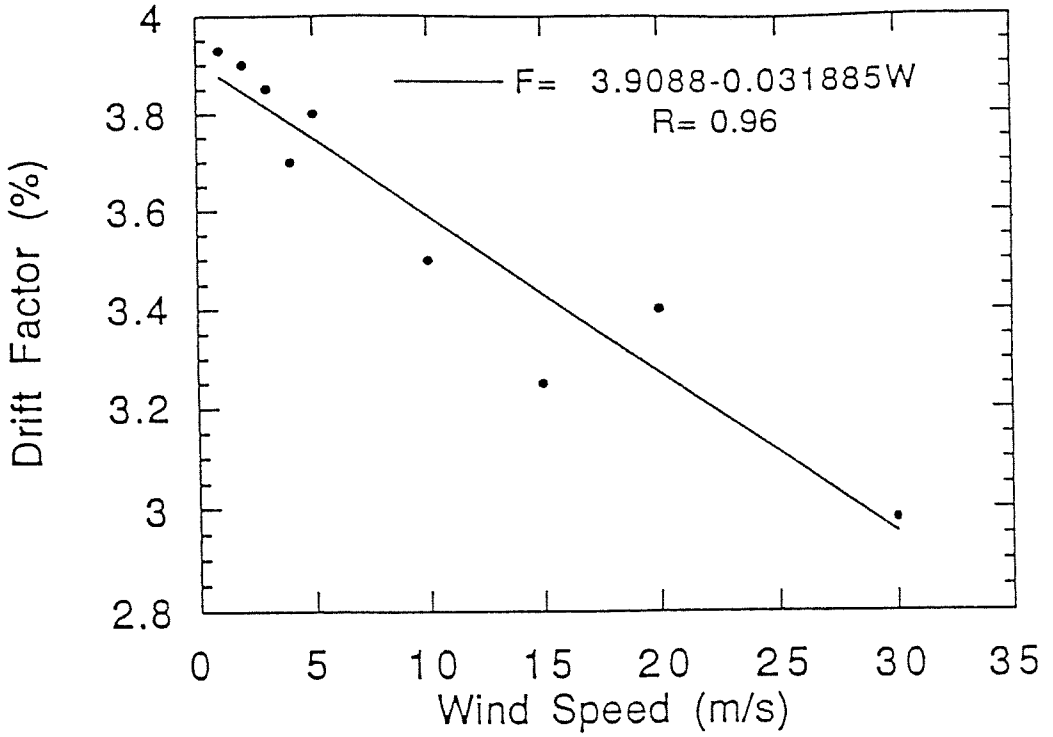

Figure 6 Model predicted, steady-state wind drift factor (solid circle) versus wind speed. Solid line represents curve fit.

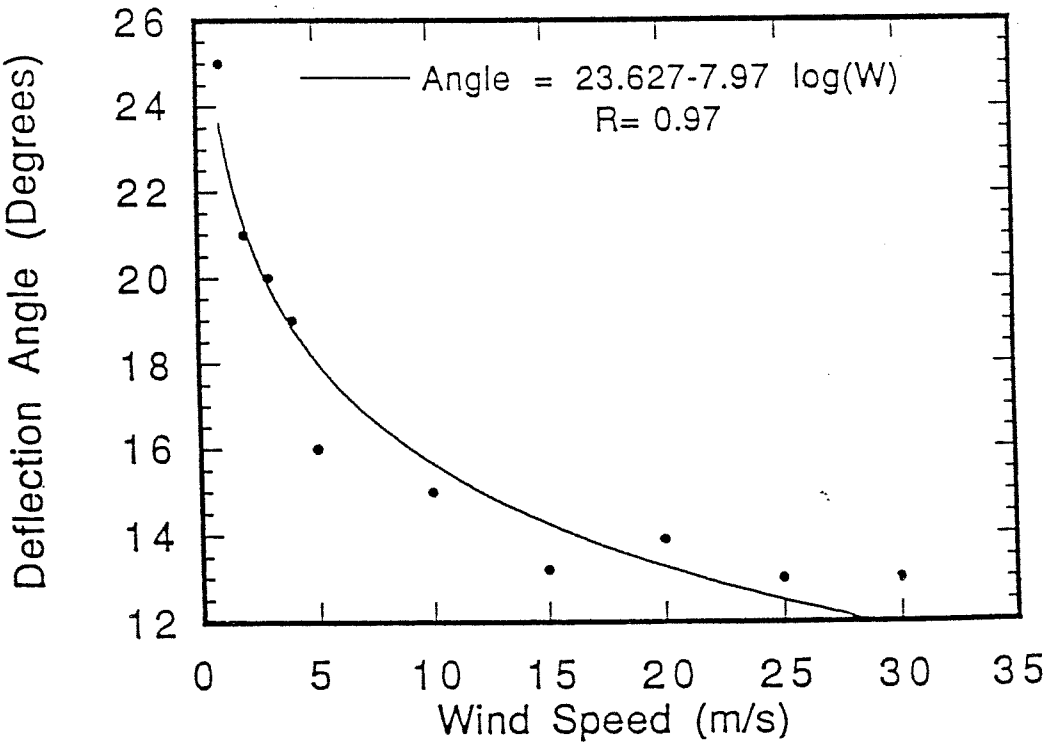

Figure 7 Model predicted, steady-state deflection angle (solid circle) versus wind speed. Solid line represents curve fit.

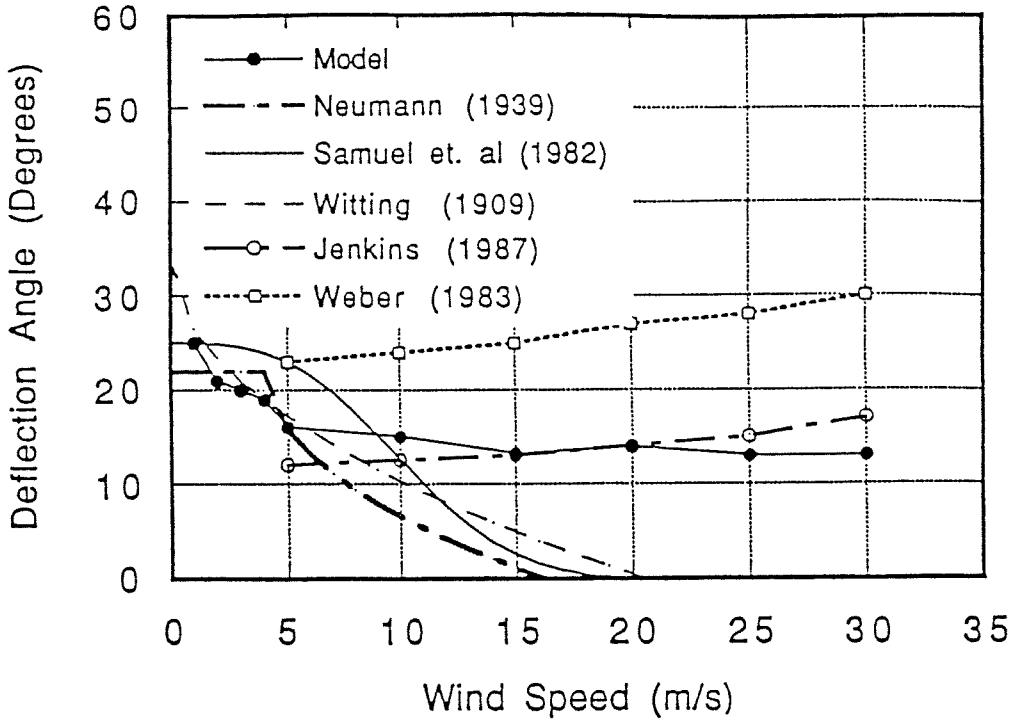

Figure 10 Comparison of the present model with Jenkins (1987) and Weber (1983) predictions and empirical formulae for the steady state deflection angle versus wind speed.

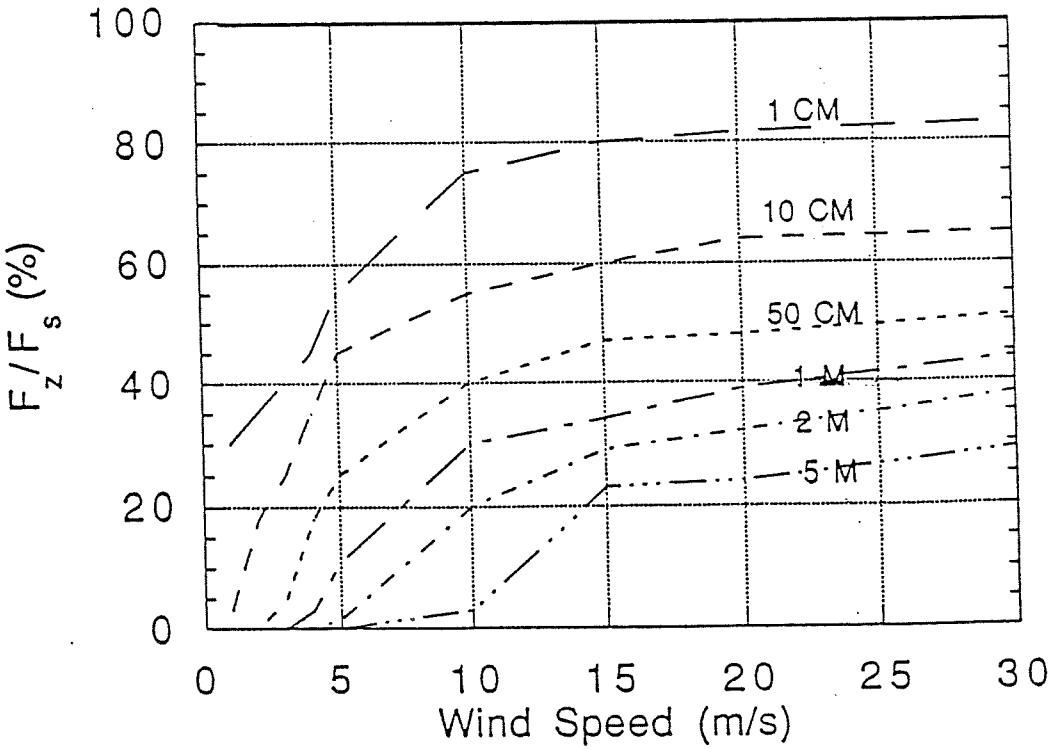

Figure 11 The ratio between the drift factor at a specific depth and at sea surface at steady state versus wind speed.

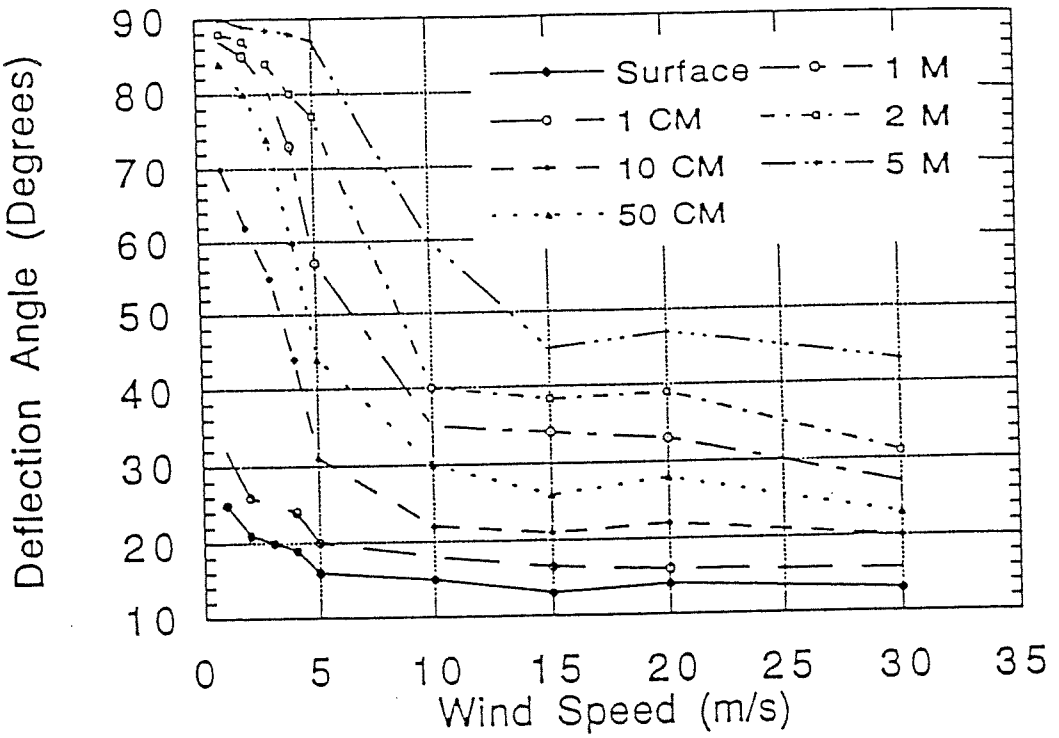

Figure 12 Model predicted steady state deflection angle with depth versus wind speed.

It is clear from studying Figures 11 and 12 that if oil is dispersed in the water column due to either breaking waves or chemical treatment that its transport velocity is significantly modified compared to the rates normally employed in spill models. In general the greater the dispersion into the water column the slower the transport and the greater the deflection from the wind direction.

To assess the importance of interaction between the wave and current field simulations with full interaction were compared to results where they were linearly superimposed. Figures 13 and 14 show the drift factor and deflection angle versus wind speed, respectively for both cases. The drift angle increases with wind speed without interaction and decreases markedly if interaction is included (Figure 13). The same behavior is observed in the deflection angle (Figure 14). Interaction between the wave and current fields results in a modification of the vertical eddy

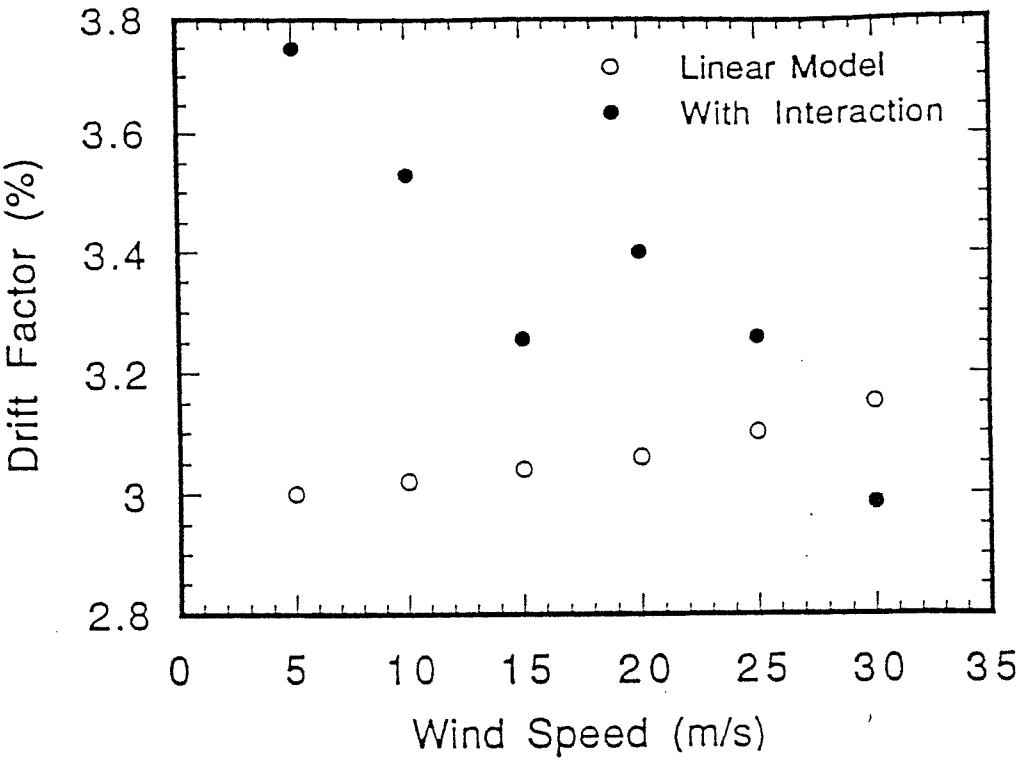

Figure 13 Model predicted drift factor versus wind speed based on fully coupled and linearly superimposed formulations.

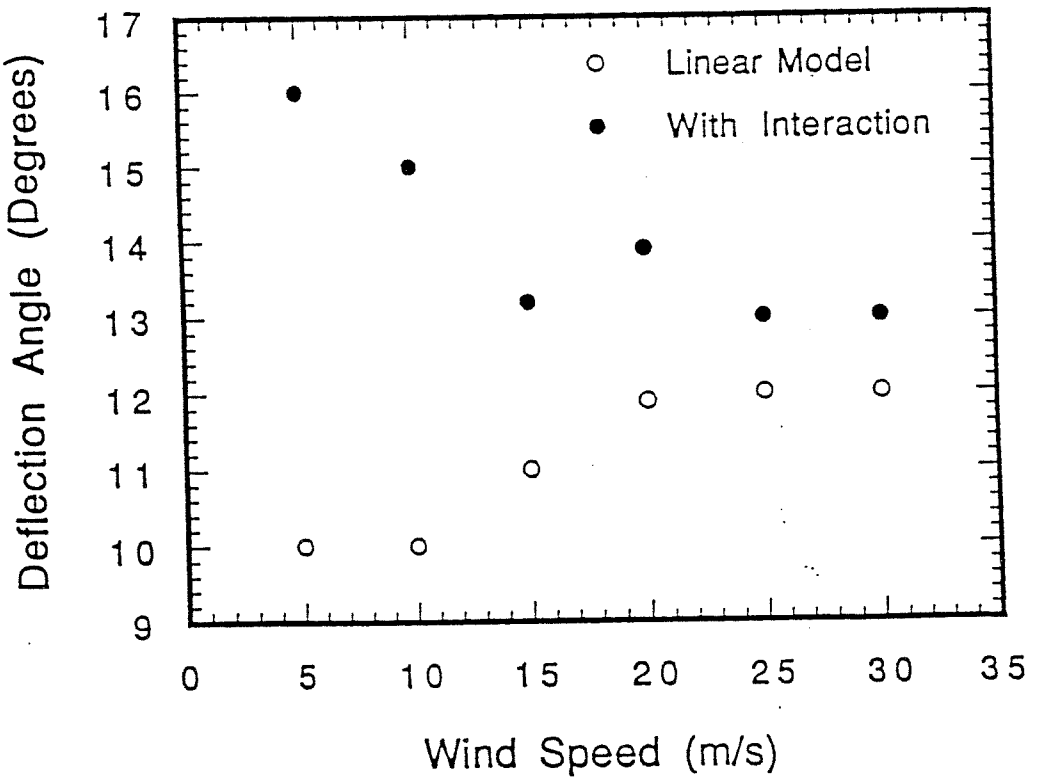

Figure 14 Model predicted deflection angle versus wind speed based on fully coupled and linearly superimposed formulations.

compute surface current velocities as well as subsurface current velocities for simulating the advection of oil droplets dispersed in the water column. During each time step the displacement of oil is calculated by numerically integrating the drift velocity over the time period. The calculation proceeds to the next time step after updating the wind and wave conditions. The trajectories were produced by the model every hour and are presented in Figure 16. Also shown are the observed surface oil spill locations for comparison at selected times (hr:min, date). The longitude and latitude scales are in minutes east of 7° East and north of 64° North, respectively. The trajectories are presented assuming the oil remains at the sea surface and at three different water depths below the sea surface; namely, 1.5H, 2.5H and 5H, where H is the significant wave height. The latter three cases attempt to estimate the trajectories for water column dispersed oil.

Figure 16a shows a comparison between the model predictions and the observed oil location for the first experiment. Observations are consistent with predictions if the oil is assumed to be transported between 1.5H and 2.5H below the sea surface. Comparison between the model predictions and oil observed locations for the second experiment are shown in Figure 16b. The observed oil position agrees well with model predictions for the drift current at the sea surface. Figure 16c shows that the results for the third experiment comparing model predictions and observed oil locations. Model predictions between the sea surface and a depth of 1.5H best represent the oil movement for the third experiment. Based on laboratory results of Delvigne and Sweeney (1988) the oil entrainment depth is predicted to be 2.1H for the first experiment and 2H for the third experiment (Youssef, 1993). These estimates are consistent with model predictions.

The results of comparisons can be explained by the fact that the oil spill behavior depends on the wind forcing, wave breaking activity and the type of oil. At wind speeds ~~below~~ 5 m/s ~~(~~in the absence of wave breaking) oil particles remain very close to the surface, as in the second experiment and hence model predictions at the sea surface are in good agreement with observations and the standard drift factor and angles. At wind speeds greater than 5 m/s wave breaking increases dramatically, as noticed in the first and third experiments. Oil at the sea surface is dispersed in the near surface waters due to turbulence generated by breaking wave events and resurfaces due to buoyant effects (Delvigne et al., 1987; Delvigne and Sweeney, 1988). Oil does not remain at the sea surface for the lifetime of the spill but instead spends

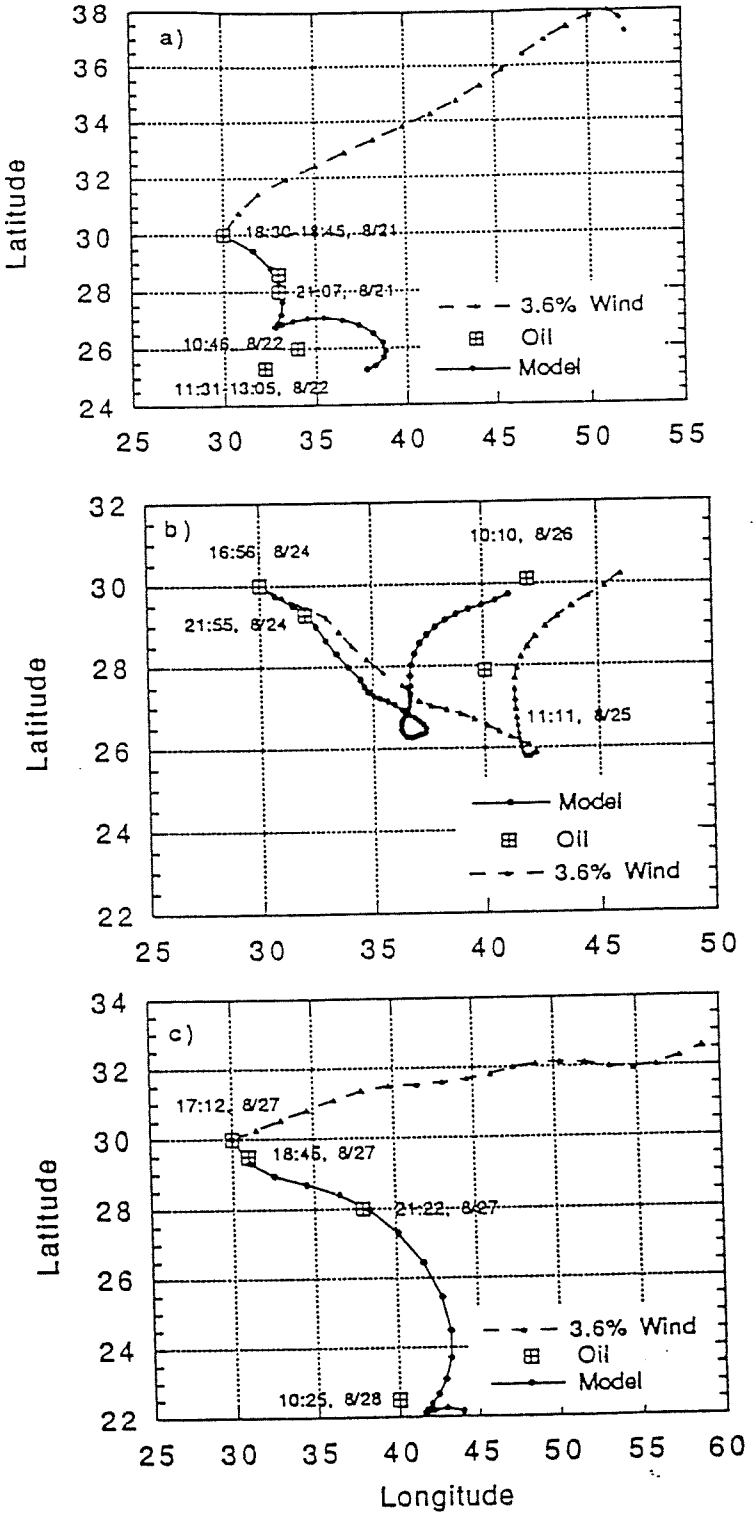

Figure 17 Comparison of observed oil location and the modeled, vertically averaged over different depths, trajectory of the oil. Also shown is a model predicted trajectory for a constant 3.6%, downwind drift. Dots denote hourly values, for the a) first, August 21, b) second, August 24, and c) third, August 27 experimental oil spills.

Model results are in general agreement with field observations and show that the drift factor and deflection angle decrease with increasing wind speed. Curve fits of the drift factor and deflection angle were performed to develop a simple methodology to estimate the drift for a specified wind speed. The curve fit to model results are restricted to steady state and assume deep water drift conditions at the sea surface. If time dependence is required the drift factor and deflection angle can be obtained from the model, as shown in Figure 1.

If oil is dispersed in the near surface waters due to breaking wave events and resurfaces due to buoyant effects its drift rate is slower than that predicted by the model at the surface due to the strong current shear near the sea surface. The lower the wind speed the stronger the vertical shear and hence the slower the transport of an oil particle located at a given depth.

Comparison between the model results and observations of experimental oil spills on the Norwegian shelf shows good agreement. The results of the present model show substantial improvement compared to the standard wind drift factor/angle procedure used in typical spill models.

REFERENCES

Ambjorn, C., "An operational oil drift model for the Baltic", Proceedings of the Symposium on Mechanics of Oil Slicks, Paris, France, 1983.

Davies, A.M., "On determining the profile of steady wind-induced currents", Applied Mathematical Modeling, v9, pp409-418, 1985.

Davies, A.M., and J.E. Jones, "Modeling turbulence in shallow sea regions", Small-Scale Turbulence and Mixing in the Ocean, editors. Nihoul C.J. and Jamart B.M.,pp 63-76, 1988.

Dean, R. and R. Dalrymple. Water wave mechanics for engineers and scientists, Prentice-Hall, Englewood Cliffs, N.J, 1984.

Huang, J.C. and F.C. Monastero, "Review of the state-of-the-art of oil spill simulation models", Final Report submitted to American Petroleum Institute, Washington, D.C, 1982.

Huang, N.E., "On surface drift currents in the ocean", Journal of Fluid Mechanics, v91, pp191-208, 1979.

Jenkins, A.D., "A theory for steady and variable wind- and wave-induced currents", Journal of Physical Oceanography, v16, pp1370-1377, 1986.

Jenkins, A.D., "Wind and wave induced currents in a rotating sea with depth-varying eddy viscosity", Journal of Physical Oceanography, v17, pp938-951, 1987.

Stolzenbach, K.D., O.S. Madsen, E.E. Adams, A.M. Pollack, and C.K. Cooper, "A review and evaluation of basic techniques for predicting the behavior of surface oil slicks", MIT Sea Grant Report No. 77-8, NTIS No. PB- 268220, 1977.

Weber, J.E., "Steady wind- and wave- induced currents in the open ocean", Journal of Physical Oceanography, v13, pp524-530, 1983.

Wu, Jin, "Sea-surface drift currents induced by wind and waves", Journal of Physical Oceanography, 13, 1441-1451, 1983.

Youssef, M., "The drift current under the action of wind and waves", Ph.D. Dissertation, Department of Ocean Engineering, University of Rhode Island, Kingston, RI, 1993.